Characterizing flat-top laser beams using standard beam parameters

S. Saghafi, M.J. Withford, and Z. Ghoranneviss

Abstract: We examine the correspondence between various models describing flat-top laser beam profiles using two standard parameters; namely, the M^2 factor and the kurtosis parameter. Numerical expressions for M^2, based on the second moment of the beam irradiance distribution in the near and far fields and for the kurtosis parameter, k, based on the fourth moment at the near field, are obtained. Plots of k in the near field versus M^2 demonstrate the similarities between the different analytical models used to describe flat-top profiles. Using the Padé approximation, a relationship between k and M^2, a new *reference* formula, is derived that predicts the values of M^2 to within less than a percent for these flattened beams. This method is then extended to define numerical expressions relating the beam parameters (i.e., M^2 and k) and the parameters describing the beam characteristic in each analytical model (model parameters). The results obtained using the Padé method are used to describe the output beam profiles for a high power copper vapour laser fitted with an unstable resonator.

PACS Nos.: 42.55.–f, 42.55.Lt, 42.60.–v

Résumé : Nous examinons la correspondance entre différents modèles qui décrivent les profiles de faisceaux laser aplatis en utilisant deux paramètres, nommément le facteur M^2 et le paramètre kurtosis. Nous obtenons des expressions numériques pour M^2 basées sur le second moment de la distribution d'irradiance du faisceau dans les champs proche et lointain et pour un paramètre kurtosis k basé sur le quatriéme moment du champ proche. Des graphiquies de k en champ proche versus M^2 démontrent les similarités entre les différents modèles analytiques utilisés pour décrire les profiles aplatis. À l'aide de l'approximation de Padé, nous obtenons une relation entre k et M^2, ce qui constitue une nouvelle formule de référence et qui prédit les valeurs de M^2 à moins d'un pourcent pour ces faisceaux aplatis. La méthode est alors généralisée pour definir des expressions numériques reliant les paramètres du faisceau (M^2 et k) avec les paramètres décrivant les caractéristiques du faisceau dans chaque modèle analytique (paramètres du modèle). Les résultats obtenus avec l'approximation de Padé sont utilisés pour décrire les profiles des faisceau de sortie d'un laser de haute puissance à vapeur de cuivre doté d'un résonateur instable.

[Traduit par la Rédaction]

Received 9 March 2005. Accepted 25 February 2006. Published on the NRC Research Press Web site at http://cjp.nrc.ca/ on 18 July 2006.

S. Saghafi.[1] Plasma-Physics Research Center Science and Research Branch Campus, Islamic-Azad University, Tehran, Iran and Environmental Scientific Research Institute, Shahid-Beheshti University, Tehran, Iran.
M.J. Withford. Physics Department, Macquarie University, Sydney, NSW 2109, Australia.
Z. Ghoranneviss. Physics Department, Pona University, Pona, India.

[1]Corresponding author (e-mail: s-saghafi@cc.sbu.ac.ir).

 doi: 10.1139/P06-012

Fig. 1. Flat-top beams in the super-Gaussian model for various beam order.

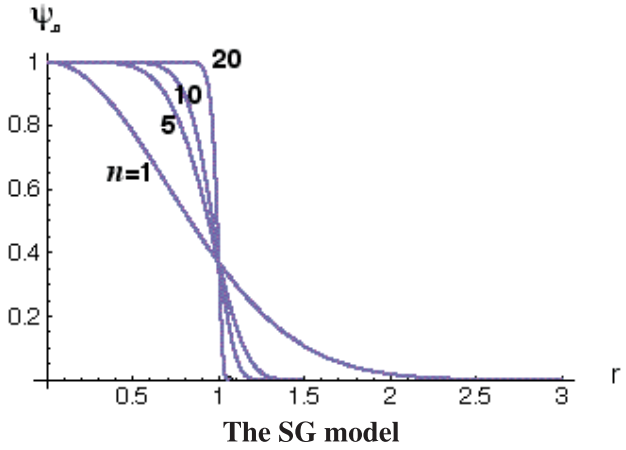

1. Introduction

The beam propagation factor M^2 is an industry standard defining laser beam quality [1–5]. Kurtosis, k, is a shape parameter, which is also often used for characterizing laser beams [6–8]. In particular, k describes the flatness of the irradiance distribution compared with normal Gaussian beams and is independent of the beam radius and divergence. These two parameters are typically used independently to quantify beam quality and flatness but it is shown here that, for a range of standard "flat-top" beams, these two factors are dependent in practice.

For many laser applications, a beam with a flat-top intensity profile (i.e., uniform irradiance over a defined cross section) is highly desired [9]. As a result, many lasers are designed to produce flat-top beams and various beam-processing techniques have been developed to obtain uniform (flat-top) beams from Gaussian and other nonuniform laser beams [10–13]. Consequently, it is important to develop theoretical models to characterize the propagation through space of flat-top beams. There are three main models, all based on the paraxial approximation, which can predict the beam diameter, intensity profile, and phase at any point along the propagation axis for beams with uniform irradiance distribution [12–15].

The first model proposed for flattened beams is the so-called super-Gaussian (SG) model [12] in which the model parameter n describes a flattened beam at the beam waist ($z = 0$). For example, the SG model describes a Gaussian beam for $n = 1$ and a flat-top beam as $n \to \infty$ (Fig. 1). The propagation of a flat-top beam in free space ($z \neq 0$) cannot be analysed using the SG model in closed form. However, a mathematical analysis was proposed by Palma et al. that describes the propagation of SG beams in free space under the paraxial approximation in terms of the Laguerre–Gauss beams [13].

In 1994, Gori [14] introduced an alternative model for describing flat-top beams, the so-called flattened Gaussian beam (referred to as FGB1 in this paper), which can change from a general Gaussian to a flat-top beam through a parameter N called the beam order. In essence, FGB1 is a finite sum of N Laguerre–Gaussian modes that are the solutions of the paraxial wave equation, thus, the model can be easily used to describe beam propagation [14]. For example, Fig. 2 shows a flat-top beam created using the FGB1 model with only five modes.

The third model developed by Sheppard et al. [15] is an alternative way of describing flat-top beam profiles (referred to as FGB2 in the remainder of this paper) in which the beam is defined at the waist to be the two-dimensional Fourier transform of the product of an Airy disc and a Gaussian. As the Airy disc propagates it produces an annular beam with a very small angle of divergence. The convolution of

Fig. 2. A flat-top beam created using the FGB1 model when $N = 5$ (i.e., $\sum_{p=0}^{N} \psi(r)$).

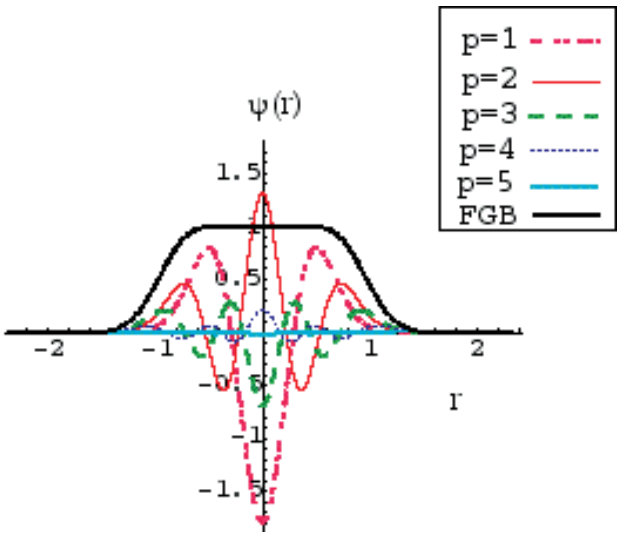

The FGB1 model

this annular beam and a Gaussian, produces flat-top beam profiles. In this case, the model parameter a determines the relative scaling of the Airy disc and the Gaussian (which adjusts the strength of the outer rings of the beam). It was demonstrated that this Fourier transform could be expressed as an infinite sum of the Laguerre–Gaussian modes.

Each of these three models has its limitations. In the SG model, the beam order (model parameter) is an integer and the irradiance profile produced by the model changes rapidly from an ideal Gaussian towards a flat-top distribution. Additionally, it cannot cover all types of uniform distributions, as when the intensity distribution of the flat-top beam most properly lies between two mode orders. In the FGB1 model, the beam order is also an integer. However, the changes in the irradiance beam profiles produced by the model parameter N is not as fast as the SG model parameter n. In the FGB2 model, the upper limit of the summation of modes is infinity, which creates mathematical difficulties in analytical characterizations of the beam.

However, each of the models has strengths and may be preferred in particular situations. To use any of these models, the model parameters n, N, and a must be defined. In this paper, a mathematical method called the Padé approximation is employed to establish the relationship between the beam parameters, M^2 and k, for flat-top beams. Then, the relationship between the beam parameters and the model parameters in each of the three analytical models is presented. These formulae enable us to switch from one model to the other depending on the application.

Finally, the validity of these results is tested against beam profile measurements of a high-power copper vapour laser with an unstable resonator.

2. The beam propagation factor (M^2) and kurtosis parameter (k)

Using the intensity moment formalism method, M^2 and k can be defined in cylindrical or rectangular coordinates. In this paper, we consider only rectangular symmetry (2D) but the results can be readily transposed to the cylindrical case (3D). M^2 describes the relationship between the beam width in the near and far fields and is invariant through propagation. If the complex field amplitude at the waist

($z = 0$) of a symmetrical beam is written as $\psi(x, 0)$, the beam propagation factor, using far-field or near-field distribution, can be defined by [16]

$$M_x^2 = \frac{\sqrt{\left(\left|\psi(x,0)\right|^2 x^2 \mathrm{d}x\right)\left(\int_0^\infty \left|\frac{\mathrm{d}\psi(x,0)}{\mathrm{d}x}\right|\mathrm{d}x\right)}}{\int_0^\infty \left|\psi(x,0)\right|^2 \mathrm{d}x} \tag{1}$$

For the sake of simplicity, we just consider the x coordinate $\left(M_x^2 = M^2\right)$.

Kurtosis is defined in terms of the second and fourth moments of the normalized field

$$k = \frac{\left(\int_0^\infty \left|\psi(x,z)\right|^2 x^4 \mathrm{d}x\right)\left(\int_0^\infty \left|\psi(x,z)\right|^2 \mathrm{d}x\right)}{\left(\int_0^\infty \left|\psi(x,z)\right|^2 x^2 \mathrm{d}x\right)} \tag{2}$$

In the following section, a detailed analysis of these two standard parameters (1) and (2) using the three different analytical models describing flat-top beam profiles is given.

3. Analysis of M^2 and k using the three flat-top models

3.1. Super-Gaussian

A commonly used model for flattened beams is called the super-Gaussian model [12] which takes the form

$$\psi(x, 0) = A \exp\left[-\left(\frac{x}{w_0}\right)^{2n}\right] \tag{3}$$

where the beam order $n \geq 1$. Equation (3) describes a Gaussian beam for $n = 1$, however, as n increases this expression describes increasingly flatter beam profiles. Exact values of M^2 and k (near-field) for the SG model can be derived by substituting (3) into (1) and (2) considering eq. (1.3.478) in the section "Definite Integrals of Elementary Function" of ref. 17

$$\int_0^\infty x^{v-1} \exp\left(-\mu x^p\right) \mathrm{d}x = \frac{1}{p}\mu^{-v/p}\Gamma\left(\frac{v}{p}\right) \tag{4}$$

where the gamma function, $\Gamma(z)$, is defined by the integral $\Gamma(z) = \int_0^\infty t^{z-1}\mathrm{e}^t \,\mathrm{d}t$

$$k = \frac{\Gamma\left(\frac{5}{2n}\right)\Gamma\left(\frac{1}{2n}\right)}{\left[\Gamma\left(\frac{3}{2n}\right)\right]^2} \qquad \text{and} \qquad M^2 = 2n\frac{\sqrt{\Gamma\left(\frac{3}{2n}\right)\Gamma\left(\frac{4n-1}{2n}\right)}}{\Gamma\left(\frac{1}{2n}\right)} \tag{5}$$

M^2 and k for beams described by the SG model, are plotted against n in Fig. 3. It can be seen that for a perfect Gaussian ($n = 1$), M^2, and k equal 1 and 3, respectively, and by increasing n these two parameters change until they approach asymptotic values of ∞ and 1.8, respectively.

Fig. 3. The values of the kurtosis parameter and the beam propagation factor versus number of modes for the super-Gaussian beam.

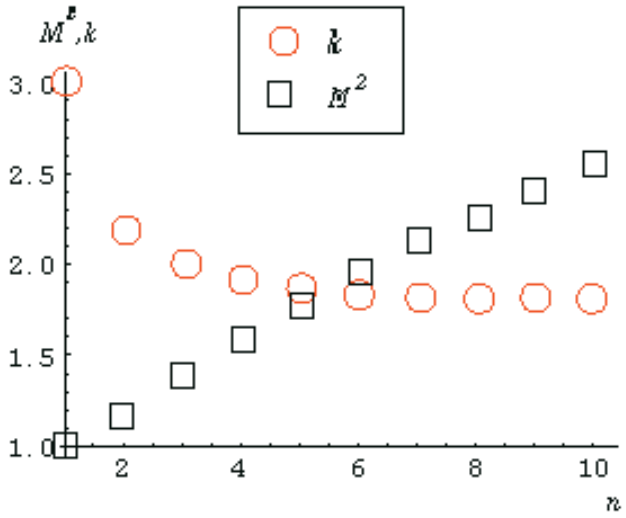

The analytical expression for the kurtosis parameter in the far field ($z \to \infty$) is given by

$$k_{\text{far field}} = \frac{\left(\int_0^\infty \left|\tilde{\psi}(\rho)\right|^2 \rho^4 \, \mathrm{d}\rho\right)\left(\int_0^\infty \left|\tilde{\psi}(\rho)\right|^2 \, \mathrm{d}\rho\right)}{\left(\int_0^\infty \left|\tilde{\psi}(\rho)\right|^2 \rho^2 \, \mathrm{d}\rho\right)^2} \tag{6}$$

where the complex field amplitude at the waist of a symmetrical beam in the far field is written as $\psi(r)$. Using the general form of even moments

$$\langle \rho^{2n} \rangle = \frac{\left(\int_0^\infty \left|\tilde{\psi}(\rho)\right|^2 \rho^{2n} \, \mathrm{d}\rho\right)}{\left(\int_0^\infty \left|\tilde{\psi}(\rho)\right|^2 \, \mathrm{d}\rho\right)} = \frac{\left(\int_0^\infty \left|\psi^{(n)} x\right|^2 \, \mathrm{d}x\right)}{\left(\int_0^\infty \left|\psi(x)\right|^2 \mathrm{d}x\right)} \tag{7}$$

where $\psi^{(n)}(x)$ is the nth derivative of $\psi(x)$.

The kurtosis parameter for the SG model in the far field, using (4), is described by

$$k_{\text{far field}} = \frac{(1-4n)^2 \, \Gamma\left(2 - \frac{3}{2n}\right) \Gamma\left(\frac{1}{2n} - 2\right)}{\left[\Gamma\left(-\frac{1}{2n}\right)\right]^2} \tag{8}$$

3.2. Gori model; FGB1

In the FGB1 model a flat-top beam is described at the waist ($z = 0$) by

$$\psi(x,0) = A\sum_{p=0}^{N} C_p L_p\left(\frac{2Nr^2}{w_0^2}\right)\exp\left[\frac{-N}{w_0^2}r^2\right]$$
$$= A\sum_{p=0}^{N}\exp\left(-\frac{Nx^2}{w_0^2}\right)\frac{\left(\frac{Nx^2}{w_0^2}\right)^p}{p!}, \qquad N = 1,2,3,\ldots \tag{9}$$

where A is a scale constant, w_0 the beam spot size, $C_p = (-1)^p \sum_{m=p}^{N}\binom{m}{p}\frac{1}{2^m}$, and N is the model parameter that in this case describes the beam order that controls the flatness of the irradiance distribution. The above equation can be recognized as a Chi-square probability function and Poisson distribution [17] that is related to the incomplete Gamma function

$$\mathrm{e}^{-\chi^2/2}\sum_{j=0}^{\frac{v}{2}-1}\frac{\left(\frac{\chi^2}{2}\right)^j}{j!} = Q\left(\chi^2|v\right) = \frac{\Gamma\left(\frac{v}{2},\frac{\chi^2}{2}\right)}{\Gamma\left(\frac{v}{2}\right)} \tag{10}$$

By using (10), the beam distribution at the waist can be written as an incomplete Gamma function

$$\Psi(x,0) = A_0\frac{\Gamma\left(N+1,\frac{Nx^2}{2}\right)}{\Gamma(N+1)} \tag{11}$$

Using eq. (6.455.1) in the section "Incomplete Gamma Function Integrals" of ref. 17

$$\int_0^\infty x^{\mu-1}\exp(-\beta x)\,\Gamma(v,ax)\,\mathrm{d}x = \frac{a^v\Gamma(\mu+v)}{\mu(\alpha+\beta)^{\mu+v}}F\left(1,\mu+v;\mu+1;\frac{\beta}{\alpha+\beta}\right) \tag{12}$$

M^2 and k (near field) can be defined as

$$M^2 = 2.0\frac{\sqrt{\Gamma\left(2N+\frac{7}{2}\right)\left(2N+\frac{1}{2}\right)!F\left(1,2N+\frac{7}{2};N+\frac{7}{2};\frac{1}{2}\right)\Big/\left(N+\frac{5}{2}\right)}}{\sqrt{3}\Gamma\left(2N+\frac{5}{2}\right)F\left(1,2N+\frac{5}{2};N+\frac{5}{2};\frac{1}{2}\right)\Big/\left(N+\frac{3}{2}\right)} \tag{13}$$

and

$$k = \frac{9}{5}\frac{\Gamma\left(2N+\frac{9}{2}\right)\Gamma\left(2N+\frac{5}{2}\right)\left(N+\frac{5}{2}\right)^2F\left(1,2N+\frac{9}{2};N+\frac{9}{2};\frac{1}{2}\right)F\left(1,2N+\frac{5}{2};N+\frac{5}{2};\frac{1}{2}\right)}{\Gamma\left(2N+\frac{7}{2}\right)^2\left(N+\frac{3}{2}\right)\left(N+\frac{7}{2}\right)\left[F\left(1,2N+\frac{7}{2};N+\frac{7}{2};\frac{1}{2}\right)\right]^2} \tag{14}$$

M^2 and k for the FGB1 model of order N in the near field are plotted in Fig. 4. Similarly to the SG case, for a perfect Gaussian M^2 and k equal 1 and 3, respectively. By increasing the beam order these two parameters change until they reach asymptotic values of infinity and 1.8. respectively. However, the rates of these changes are not as fast as those of the SG model. The kurtosis parameter for the FGB1 model in the far field, is derived as

$$k_{\text{far field}} = \frac{(8N+3)\Gamma\left(2N+\frac{5}{2}\right)F\left(1,2N+\frac{5}{2};N+\frac{5}{2};\frac{1}{2}\right)}{(2N+3)(4N+1)\left(2N+\frac{1}{2}\right)!} \tag{15}$$

The propagation of a flat-top beam described by the FGB1 model is discussed in details in refs. 18 and 19.

Fig. 4. The values of the kurtosis parameter and the beam propagation factor versus number of modes for the FGB1.

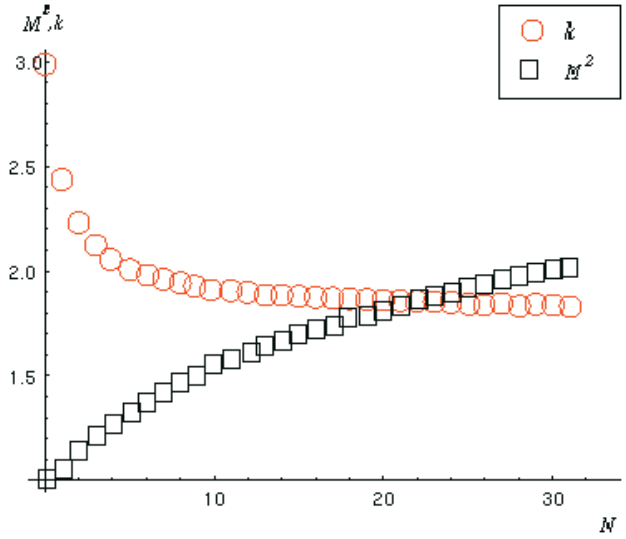

3.3. Sheppard et al. model; FGB2

The FGB2 model is defined at the waist to be the two-dimensional Fourier transform of the product of an Airy disc and a Gaussian. This was shown to give [15]

$$\psi(x,0) = \sum_{p=0}^{\infty} A_p(a) L_p\left(\gamma^2 x^2\right) \exp\left[\frac{-\gamma^2 x^2}{2}\right] \tag{16}$$

with $\gamma = ka\sin\alpha$ where $k = 2\pi/\lambda$, α is the semi-angle of divergence (assumed to be small so that the paraxial approximation holds), and a is this model parameter. Finally, $A_p(a)$is given by

$$A_p(a) = \exp\left(-\frac{1}{4a^2}\right) \sum_{q=p+1}^{\infty} \frac{4a^2}{q!}\left(\frac{1}{2a}\right)^{2q} = 4a^2\left[1 - F_p\left(\frac{1}{2a}\right)\right] \tag{17}$$

where

$$F_p(x) = \exp\left(-x^2\right) \sum_{q=0}^{p} \frac{x^{2q}}{q!} \tag{18}$$

$F_p(x)$ is exactly the flattened Gaussian profile introduced by Gori [14] but here it appears in the amplitude of the various Laguerre–Gaussian modes.

The numerical values of M^2 and $k_{\text{near field}}$ for the field described by (16) are plotted in Fig. 5 for different values of $1/a$.

The analytical expressions derived for M^2 and k depend on the model parameters (e.g., n, N, and a in SG, FGB1, and FGB2, respectively). The development of a parametric formula that is independent of the model parameter in each model and describes the relationship between the beam parameters (M^2 and k) is the subject of the following sections. To calculate M^2 and k, a mathematical method called the Padé approximation is employed.

Fig. 5. The values of the kurtosis parameter and the beam propagation factor versus number of modes for the FGB2.

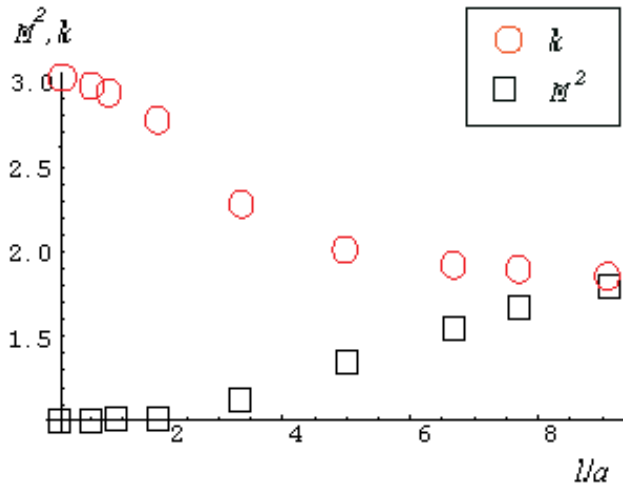

4. Padé approximants

When the value of a function such as $\psi(x)$ is known at a set of points, and we do not know the analytical expression for this function, there are methods that help us to estimate the value of $\psi(x)$ at any arbitrary point. There is a related class of approximation theorem involving the interpolation and extrapolation method fitting a smooth curve through a set of data points by an approximating function. Thus, the value of $\psi(x)$ at any arbitrary point can be defined by deriving a parametric expression.

The most common approximations for a function are polynomials, however, the functions considered in the current paper cannot be approximated by polynomials and alternative methods must be chosen. One of these methods of approximation is the Padé approximation.

Assuming a field described by a power series

$$\psi(x) = \sum c_m x^m \tag{19}$$

the Padé approximant to $\psi(x)$ is a rational function (the ratio of polynomials) described by

$$P(x) \equiv \frac{\sum_{k=0}^{N} e_k x^k}{1 + \sum_{k=1}^{M} b_k x^k} \tag{20}$$

Because these functions only use the elementary arithmetic operations, they are very easy to evaluate numerically. *The polynomial in the denominator allows one to approximate functions that have rational singularities*; for this reason it is frequently useful in numerical work to approximate a given function by a rational function.

If $\psi(x)$ is defined as a series, then the first and second terms can be kept while the higher order terms are replaced by the term derived using the Padé approximation. This may be done by multiplying $\psi(x)$ by the denominator of (20), and equating all powers of x that have either c's or b's in their coefficients.

Fig. 6. The parametrical expressions and analytical data for the SG, FGB1, and FGB2 models.

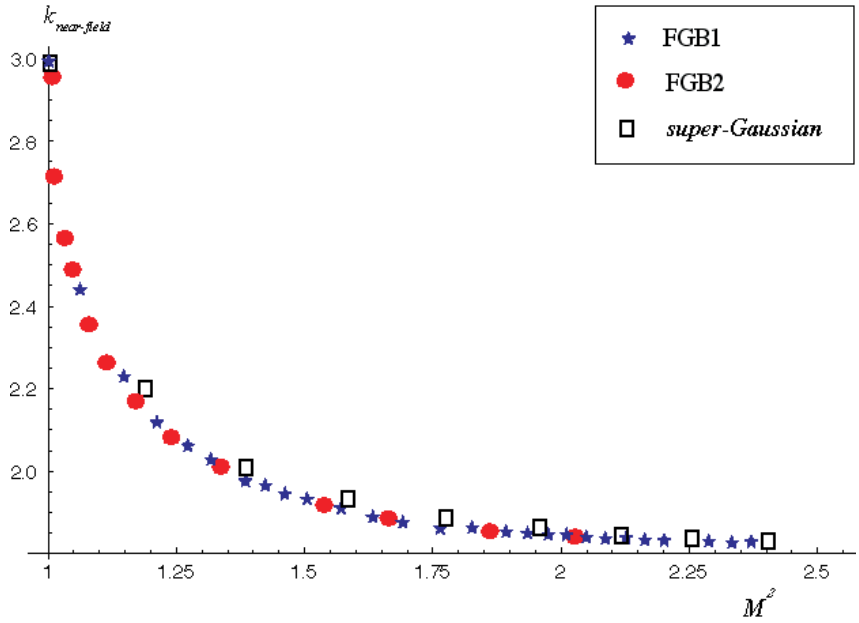

5. Relationship between M^2 and k for three different models describing flat-top beams

In practice, there are instruments that measure the beam propagation factor for which the beam widths in the near field ($z = 0$) and the far field are usually required. By comparison, the kurtosis factor for different beam profiles is usually determined individually and there are few instruments capable of measuring k. However, both these beam parameters are relevant to laser beam characterization. In the following sections, we will demonstrate that there is a global relationship between the beam parameters for all flat-top beams and the model parameters of the various models describing flat-top beams.

Different methods for determining the beam propagation factor and the kurtosis parameter have been developed and discussed in detail elsewhere [2–8]. However, the analytical expressions derived for these parameters in the previous section depend on the model parameter such as n, N, and a. Here, instead of considering the beam propagation factor and kurtosis parameter individually, the changes of k with respect to M^2 are considered.

5.1. The correspondence between M^2 and k for the SG model

The changes in values of k with respect to M^2 in the SG model are plotted in Fig. 6. In the SG model, for $n = 1$ and ∞, $k = 3$ and 1.8 (note this appears as $\frac{9}{5}$ in subsequent equations), and $M^2 = 1$ and ∞, respectively. The analytical expression for kurtosis and M^2 (5) can be written as a power series.

In particular, the kurtosis parameter can be approximated as

$$k_{n\to\infty} = \frac{9}{5} + \frac{2\pi^2}{15x^2} - \frac{4\left(\pi^2 + 18\text{zeta}[3]\right)}{45x^3} + \frac{4\left(-5\pi^2 + 3\pi^4 + 90\text{zeta}[3]\right)}{225x^4} + O(5) \tag{21}$$

or

$$k_{n\to 1} \approx 3 - \frac{2x}{\sqrt{\pi^2 - 8}} + \left(\frac{3}{2} - \frac{2\left(\pi^2 - 7\text{zeta}[3]\right)}{\left(\pi^2 - 8\right)^2}\right)x^2 + O(3) \tag{22}$$

where $x = \sqrt{M^8 - 1}$ and zeta[3] = 1.2020 is the Riemann zeta function with integer arguments (in this case 3) that arise in evaluating various sums and integrals. $O(t)$ indicates components of order t and higher.

Shortening the series described by (21) and (22) by the second component, they become

$$k_{n\to\infty} \approx \frac{9}{5} + \frac{2\pi^2}{15x^2} \tag{23}$$

and

$$k_{n\to 1} \approx 3 - \frac{2x}{\sqrt{\pi^2 - 8}} \tag{24}$$

Considering the second part of (23) and (24) (the first component of (23) and (24) gives the exact value of the kurtosis factor when $M^2 = \infty$ and 1, respectively). However, to obtain a parametric relationship between these two standard parameters for intermediate values of n, the Padé approximation for this situation is considered as

$$P(x) \equiv \frac{c_0}{1 + b_1 x + b_2 x^2} \tag{25}$$

The coefficient in (25) can be obtained by replacing $P(x)$ with the approximated expressions for kurtosis (23) and (24), multiplying them by the denominator and then solving these equations. Finally, the parametrical expression for kurtosis (SG model) can be calculated as

$$K_{\mathrm{SG}} = 1.8 + 1.2 \Big/ \left[1 + 1.079(M^8 - 1) + 1.2189\sqrt{(M^8 - 1)}\right] \tag{26}$$

Following the same method, M^2 can be given in term of k

$$M^2_{\mathrm{SG}} = M^2_s = \sqrt{\frac{\frac{6}{5} - \sqrt{k - \frac{9}{5}} + \left(k - \frac{9}{5}\right)}{\left[1 + 0.185\sqrt{k - \frac{9}{5}} - 0.01\left(k - \frac{9}{5}\right)\right]\sqrt{k - \frac{9}{5}}}} \tag{27}$$

It must be noted that even though the higher order terms in our approximation have been neglected, the value of the beam propagation factor for an arbitrary k can be predicted by (27) to within ± 0.09 error compared with the value given by the numerical calculation (e.g., for $k = 3$ (when $n = 1$), $M^2 = 1.0001$).

5.2. The correspondence between M^2 and k for the FGB1 and FGB2 models

Considering the changes of k (5), (14), and (16) with respect to M^2 (5), (13), and (16) in the FGB1 and FGB2 models, both models reveal similar relationships between k and M^2 factors (Fig. 6). Thus, following the method described in the previous section, a parametric plot of kurtosis versus M^2 can be fitted to the data points of both models that is described by

$$k_{\mathrm{FGB1,2}} = 1.8 + 1.2 \Big/ \left[1 + \left(1.5708(M^8 - 1) + 1.3713\sqrt{(M^8 - 1)}\right)\right] \tag{28}$$

where $k_{\mathrm{FGB1,2}}$ is the predicted value of the kurtosis factor in the FGB1 and FGB2 models for a given value of M^2 where $\Delta(K) \leq 0.007$, and $\Delta k = |k_{\mathrm{FGB}} - k|$. Clearly, excellent agreement can be presented between the data obtained using numerical calculation (1), (2), (13), (14), and (16) and the parametric curve that is a best fit interpolation (28) in Fig. 7.

Following the same method, M^2 for FGB1 and FGB2 can be given in term of k

$$M^2_{\mathrm{FGB1,2}} = \sqrt{\frac{0.955 - \sqrt{k - \frac{9}{5}} + \left(k - \frac{9}{5}\right)}{\left[1 - 0.4\sqrt{k - \frac{9}{5}} + 0.3\left(k - \frac{9}{5}\right)\right]\sqrt{k - \frac{9}{5}}}} \tag{29}$$

Fig. 7. A comparison between the analytical data for the FGB2 model and the generalized parametric formula derived using the Padé approximation (28).

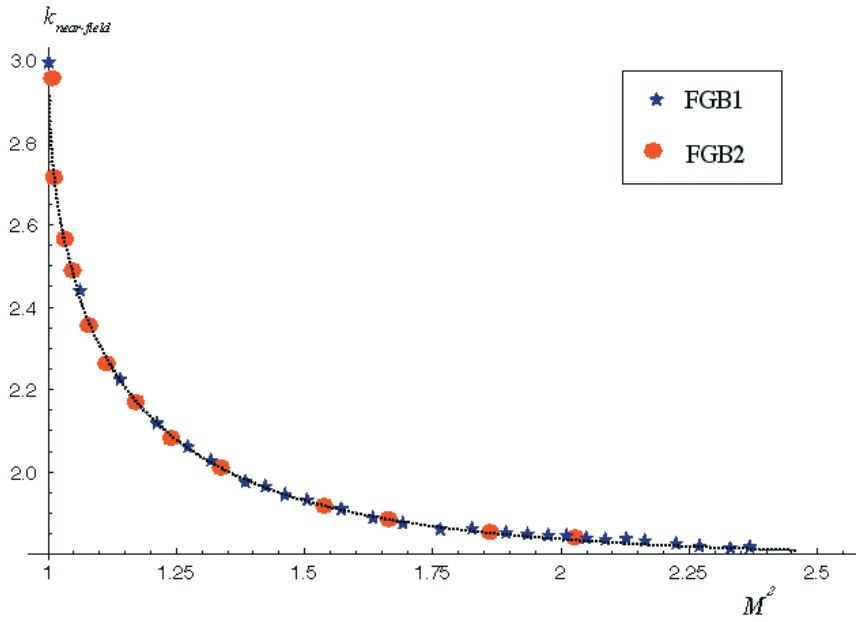

5.3. The correspondence between M^2 and k through the reference formula

Finally, considering all data, a reference curve lying between the curves described by (26) and (28) is introduced as

$$K_{\text{ref}} = 1.8 + 1.2 \Big/ \left\{ 1 + 1.29 \left[-1 + \left(M^2 \right)^4 \right] + 1.07 \sqrt{\left[-1 + \left(M^2 \right)^4 \right]} \right\} \tag{30}$$

The kurtosis factor predicted by (30) for an arbitrary M^2 is related to the values given by the three different models through $K_{\text{SG}} = K_{\text{ref}} + \Delta k$ and $K_{\text{FGB}} = K_{\text{ref}} - \Delta k$, where $0 \leq \Delta k \leq 0.01$, and in which K_{SG} and K_{FGB} represent the kurtosis parameter for the SG and FGB1-2 models, respectively.

Again, the same method is employed to derive a reference formula for M^2 in term of k

$$M^2_{\text{ref}} = \sqrt{\frac{1.15 - \sqrt{k - 1.8} + (k - 1.8)}{(1 + 0.24\sqrt{k - 1.8} - 0.145(k - 1.8))\sqrt{k - 1.8}}} \tag{31}$$

Also for all three models describing flat-top beams, the relationship between M^2 and k or vice versa can be replaced by (30) or (31), and it is possible to replace one expression with the other without significant error.

6. Defining the model parameters of the SG, FGB1, and FGB2 models using M^2 and k

To employ a model to predict a real flat-top laser beam profile, parameters such as beam width at the waist, the wavelength, and particularly the model parameter (beam order) must be known. The model parameter can be approximately defined by measuring the beam irradiance distributions of the real beam in a number of planes (from the near to the far field) and fitting these data to various analytical beam

profiles produced by different beam orders. Alternatively, a parametric formula in terms of k or M^2 can be obtained, using the Padé approximation method, to predict the model parameters. The second solution is quick, convenient, and accurate. In the following sections, expressions describing the model parameter in three different models (n, N, and a) are given in terms of the beam parameters (k and M^2). Depending on the application and practical preferences, either k or M^2 can be used. For example, the data measured in the near field are sufficient to calculate the kurtosis factor and the beam profile can be characterized at any other point. However, the most common laser beam analyzer instruments are able to calculate M^2 for flat-top beams (using the far field as well as the near field). In the following section, we will demonstrate that by substituting one of these beam parameters in the analytical expressions that will be obtained for the model parameters, researchers will be able to choose the appropriate model to analyse and characterize a real laser beam (examples will be demonstrated in the experimental section).

6.1. The SG model

As in Sect. 4, the SG model will be considered initially. Considering the series theorem, n can be approximated by two series as a function of M^2

$$n = \frac{1}{2} + \frac{3\sqrt{\left(M^2\right)^4 - 1}}{2} + \frac{\frac{3}{4} - \frac{\pi^2}{9}}{\sqrt{\left(M^2\right)^4 - 1}} + \frac{-\frac{3}{16} + \frac{\pi^2}{54} - \frac{4\pi^4}{243} - \frac{4\text{zeta}[3]}{9}}{\left[\sqrt{\left(M^2\right)^4 - 1}\right]^3} + \frac{2\left(\pi^2 + 6\text{zeta}[3]\right)}{27\left[\left(M^2\right)^4 - 1\right]} + O\left\{\frac{1}{\left[\left(M^2\right)^4 - 1\right]}\right\}^{3/2} \tag{32}$$

and

$$n = 1 + \frac{\sqrt{M^8 - 1}}{\sqrt{\pi^2 - 8}} + O\left(\sqrt{M^8 - 1}\right)^2 \tag{33}$$

For large M^2, the beam order can be approximated using (32), and (33) enables us to predict the values of n for a small M^2. Considering the Padé method and (32), and (33)

$$P(x) \equiv \frac{c_0 + c_1 x + c_2 x^2}{1 + b_1 x} \tag{34}$$

a new formula for beam order in terms of M^2 is obtained

$$n = 1 + \frac{\sqrt{\left(M^2\right)^4 - 1}}{\sqrt{\pi^2 - 8}} + \frac{\left[\left(M^2\right)^4 - 1\right]}{\left(\pi^2 - 8\right)^2\left[1 + \frac{5\sqrt{\left(M^2\right)^4 - 1}\left(\pi^2 - 7\text{zeta}[3]\right)}{2\left(\pi^2 - 8\right)^{3/2}\left(-2 + 3\sqrt{\pi^2 - 8}\right)}\right]} \tag{35}$$

The same method can be used to obtain the correspondence between the beam orders and the kurtosis factor

$$n = \frac{1 + (3 - k)^2 + \frac{5(3-k)}{3\sqrt{\pi^2 - 8}}}{\sqrt{\left(\frac{5}{6} + (3 - k) + (3 - k)^2 + 2(3 - k)^3\right)\left(k - \frac{9}{5}\right)}} \tag{36}$$

Fig. 8. A comparison between data describing the changes of N versus M^2 for the FGB1 model and the generalized parametric formula described by (38).

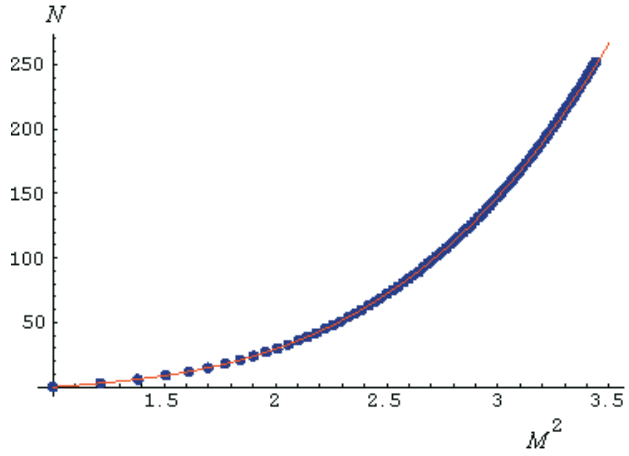

6.2. The FGB1 model

Considering (11) and employing the Padé approximation as

$$P(x) \equiv \frac{c_0 + c_1 x + c_2 x^2 + c_2 x^2}{1} \tag{37}$$

a parametric expression for the beam order in FGB1 is obtained

$$N = 12\left(M^2 - 1\right) + 2.5\left(M^2 - 1\right)^2 + 14\left(M^2 - 1\right)^3 \tag{38}$$

The change in N as M^2 increases is plotted in Fig. 8.

Using the Padé method and (12), the beam order can be defined in terms of the kurtosis factor for FGB1 with an error of $\Delta N = \pm 2$ as

$$N = \sqrt{\frac{\frac{20}{13}}{\left(k - \frac{9}{5}\right)^2} - \sqrt{k - \frac{9}{5}} + \left(k - \frac{9}{5}\right)} \tag{39}$$

By measuring the beam intensity profile at $z = 0$, the kurtosis factor can be determined using (2). Thus, researchers can easily define the beam order (i.e., N) using (39).

6.3. The FGB2 model

Due to mathematical difficulty and a lack of analytical expressions for the beam parameters in FGB2, establishing the series theorem is a difficult task. However, using alternative numerical methods such as the curve of best fit, a parametric formula can be obtained

$$a = \frac{1}{15} + \exp\left(-\frac{10}{3.5}\sqrt{\left(M^2\right)^2 - 1}\right) + 2.5\exp\left(-10\sqrt[4]{\left(M^2\right)^2 - 1}\right) \tag{40}$$

and plotted in Fig. 9. Alternatively, considering (2), (16), and (20), for a given kurtosis at $z = 0$ we are easily able to define a

$$a = -7.637k + 9.953k^2 - 4.2635k^3 + 0.611k^4 \tag{41}$$

7. Application to describe the propagation of a real flat-top laser beam

As has been discussed earlier, three different models describing flat-top beams can be employed for characterizing the propagation of a real laser beam along the z-axis. To do this, the model parameters describing FGB2 and FGB1 beam characteristic, namely, n, N, and a in the SG, FGB1, and FGB2 models, respectively, must be determined. This can be done through two different approaches.

The kurtosis factor can be calculated in just one plane using the measured beam intensity profile at $z = 0$ (corresponding to the plane immediately behind the output coupler) and (2), (36), (39), or (41) can then be employed to determine the model parameters. The *reference formula* given by (31) can also be used to estimate the beam propagation factor M^2.

Alternatively, in various instruments that are commonly used by laser physicists, M^2 can be determined automatically, by measuring the beam intensity profiles at different points. Therefore, (35), (38), and (40) enable us to determine the model parameters. It must be noted that a difference between the predicted angle of divergence in the paraxial approximation theorem and in the experimental regime can occur. A useful equation used by experimentalists to derive the beam propagation factor is [20]

$$M^2_{\text{exp}} = \frac{4\pi d_0 D_0}{\lambda f} \tag{42}$$

where f is the focal length of the lens used to focus the beam into the far field, d_0 and D_0 are the effective beam diameters of the beam in near and far field. The angle of divergence in the paraxial regime is described in ref. 21

$$\theta = \frac{4\lambda M^2}{\pi d_0} \tag{43}$$

Replacing M^2 in (43) by its experimental or theoretical values, the angle of divergence in the theoretical or experimental regimes can be predicted. In an ideal system, these two values are identical, however, real laser beams (such as those employed in the following experimental section) are not generally perfect. In such cases, the theoretically determined angles of divergence are usually smaller than those predicted experimentally.

8. Experimental analysis

8.1. Experimental set up (near field)

The laser used in this study was a conventional 20 W copper vapour laser (CVL) (active volume 25 mm diameter $\times$ 1 m long) with a thyratron-switched excitation circuit consisting of two stages of pulse compression. The laser was operated with a 2% H_2–Ne buffer gas (buffer gas pressure of 40 Torr) at a pulse repetition frequency of 10 kHz [22].

The optical resonator was a negative branch on-axis unstable, confocal resonator formed by a $R_1 = 4$ m high reflector (50 mm diameter) at one end and a 50% reflecting mirror located at 45° to the axis, which directed the centre of the beam onto an auxillary reflector [22]. The auxillary reflector had the radius of curvature (R_2) of 5 cm, corresponding to a resonator magnification (R_1/R_2) of $M = 80$. The optical resonator, shown in Fig. 10 produces a top-hat beam profile.

The pulse-averaged near-field intensity profile of the green component of laser output (at $z = 0$, corresponding to the plane immediately behind the output coupler) was recorded by using a dichroic filter to reject the yellow component and imaging via a $f = 160$ mm achromatic lens onto the CCD camera of a Spiricon laser beam analyzer. The beam width at $z = 0$ is 25 mm.

8.2. Experimental set up (far field)

Pulse-averaged far-field intensity profiles of the green laser output were examined by taking a low-power sample of the output (via reflections from several wedges), and then bringing this sample to focus

Fig. 9. A comparison between data describing the changes of a versus M^2 and the generalized parametric formula described by (40).

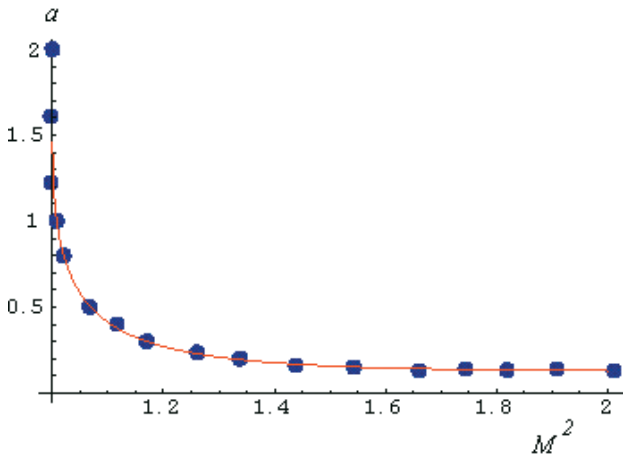

Fig. 10. The oscillator used in the copper vapour laser to produce a flat-top beam.

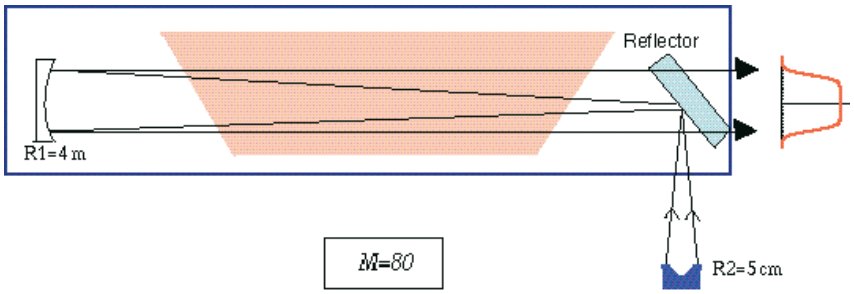

using a $f = 750$ mm achromatic doublet lens. A magnified image of this focal spot was produced on the CCD camera of the laser beam analyser using a $f = 75$ mm singlet lens. The effective beam width was determined to be 50 μm.

9. Results and discussion

A near-field intensity profile of the CVL recorded at $z = 0$ is plotted in Fig. 11. Considering (2) and a best fit to the measured intensity of beam profiles at $z = 0$, we calculate the kurtosis parameter as 1.822 ± 0.002. As is illustrated in Fig. 6, for a given M^2 the SG model always predicts a larger k compared with the FGB1 and FGB2 models. Note that the upper limit in 1.822 ± 0.002 estimates the values given by the SG model (1.824) while the lower limit approximates the kurtosis values in the FGB1 and FGB2 models (1.820). By substituting this value for k in the (36), (39), and (41), the model parameters (n, N, and a in SG, FGB1, and FGB2 models, respectively) can be obtained as 10, 62, and 0.07, respectively. The reference formula (31) is then used to estimate M^2 as 2.5 ± 0.1. Considering the theoretical value of M^2, the angle of divergence in the paraxial regime is $65.1 \pm 1.2\mu$ rad. To define M^2 experimentally the intensity profile in the far field was also measured.

The M^2 for this laser is determined to be 2.52 ± 0.11, which is in good agreement with the result predicted by the reference formula. Furthermore, the upper limit gives the closest value to the value predicted by the SG model while the closest approximation to the values given by the FGB1 and FGB2 models is given by the lowest limit. The angle of divergence, measured experimentally as 66.7 μrad, is

Fig. 11. The near field intensity profile at $z = 0$ (corresponding to the plane immediately behind the output coupler of the copper vapour laser).

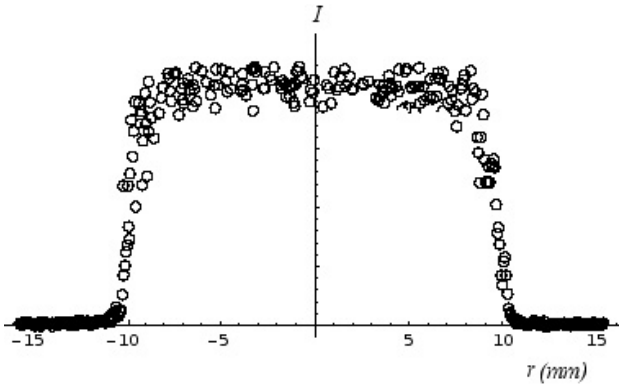

also in excellent agreement with that calculated using the reference formula and one near-field intensity profile (the difference is about 2%). Using this information, the beam parameter for each of the three analytical models describing flat-top beams can be obtained. For example, for the SG model, using the upper limit of 2.52 ± 0.11 as 2.63, the model parameter n, is approximated using (27) and (35) as $n = 10$. For the FGB models model, using the lowest limit of 2.52 ± 0.11 as 2.41, the beam parameter in the FGB1 model, N, is defined as 62 and similarly, a in the FGB2 model is 0.07.

It can be seen that, there is an excellent agreement between the results obtained using either of the two approaches.

As it can be seen in Figs. 6–7, the FGB1 model is, in general, the most convenient to use except for a comparatively high value of k ($k \geq 2.1$) where the FGB2 model is most appropriate, because

(1) it can be defined as a superposition of higher order modes in cylindrical coordinates, thus, the analytical concepts of beam diameter, and radius of curvature can be adopted,

(2) the finite limit in the summation of modes makes mathematical evaluation adequately simple,

(3) the slowness of change in the shape of the irradiance distribution, caused by the increase in N, is a particular advantage of the FGB1 model compared with the SG model,

(4) and the FGB1 model is compatible with the FGB2 model for cases where the latter is most appropriate (high k).

For the experimental data of Fig. 11, the kurtosis parameter was measured as 1.822, for which the FGB1 model is most appropriate. Using the corresponding FGB1 beam order of $N = 62$, eq. (3) from ref. 22 is used to fully characterize the propagating beam and predict the beam profiles at any arbitrary point along the z-axis. Figure 12 shows the comparison between the theoretical predictions using the FGB1 model for $N = 62$ and the experimental measurements of the real beam profile at various points along the propagating path.

We see, for example, at $z = 1$ m two small peaks appear on the shoulders of the intensity profile. At $z = 2$ m, the peaks on the shoulders become more pronounced, and at $z = 5$ m further distortion becomes apparent. At $z = 15$ m, three peaks can be seen with the central peak the most dominant. Excellent agreement is also observed between the calculated and experimental far-field intensity profiles.

Fig. 12. The comparison between the theoretical predictions and experimental measurements at $z = 0$, 1, 2, 5, 15 m and the far field.

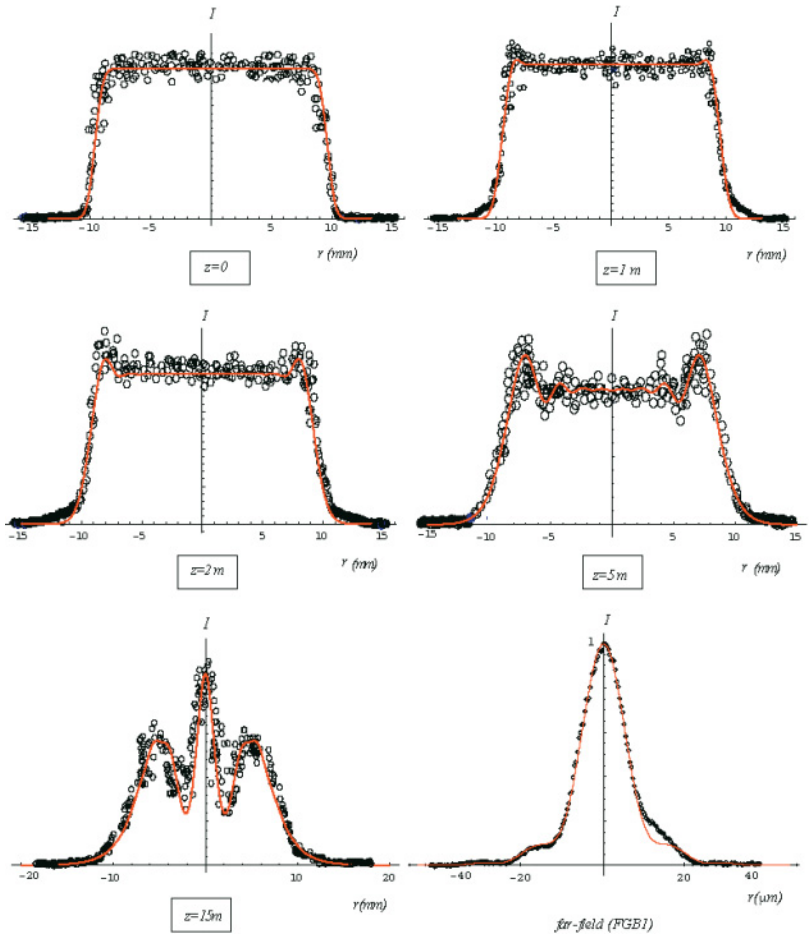

10. Conclusion

Three analytical models describing beams with uniform irradiance distributions have been considered. Based on the second- and fourth-moments formalism, analytical expressions for two standard parameters (i.e., M^2 and k) were derived. Using the Padé method a *reference formula* linking the beam propagation factor M^2 and the kurtosis parameter k has been obtained.

Using the same method, a relationship between beam parameters for these three models (i.e., N, a, and n, respectively) was derived. The kurtosis parameter can be determined measuring the beam profile in the near field ($z = 0$). This allows for a highly accurate prediction of the parameters required for these analytical models to be made.

Thus, a single near-field profile measurement allows a flat-top beam profile to be predicted in any arbitrary plane along the propagation axis to the far field. In addition, a second profile measurement (far field) enabled us to calculate the experimental beam propagation factor M^2 (and related angle of divergence) and compared them with the estimated values using measured k and the *reference formula*.

We believe this approach to flat-top laser beam characterization can be very useful in a range of laser applications.

Acknowledgment

The authors thank Professors Colin Sheppard and Greg Forbes for useful discussions about the flat-top beams and Padé method. The authors also thank both Islamic-Azad University, Research and Science Foundation and Macquarie University.

References

1. M. Sasnett. Physics and technology of laser resonators. Adam Hilgers, Bristol. 1989. p. 132.
2. A.E. Siegman. Proc. SPIE, **1224**, 2 (1990).
3. T.F. Johnston, Jr. Laser Focus World, **26**, 173 (1990).
4. ISO/TC 172/SC9/WG1/N56. Optics and optical instruments: Test methods for laser beam parameters.
5. A.E. Siegman. Proc. IEEE, **53**, 267 (1965).
6. R. Martinez-Herrero, G. Piquero, and P.M. Mejias. J. Opt. Commun. **115**, 225 (1995).
7. R. Martinez-Herrero, P.M. Mejias, M. Sanchez, and J.L.H. Neira. J. Opt. Quantum Electron. **24**, 1021 (1992).
8. M. Scholl and G. Herizger. Proc. SPIE, **2375**, 130 (1995).
9. W. Fushun. Proc. SPIE, **3274**, 306 (1998).
10. D. Shafer. J. Opt. L. Tech. **14**, 159 (1982).
11. V. Kermene, A. Saviot, M. Vampouille, B. Colombeau, and C. Froehly. Opt. Lett. **17**, 859 (1992).
12. S. De, P. Laporta, V. Magni, and O. Svelto. IEEE J. Quantum. Electron. **26**, 1172 (1988).
13. C. Palma and V. Bagini. Opt. Commun. **111**, 6 (1994).
14. F. Gori. Opt. Com. **107**, 335 (1994).
15. C.J.R. Sheppard and S. Saghafi. Opt. Commun. **132**, 144 (1996).
16. S. Saghafi and C.J.R. Sheppard. Opt. Commun. **153**, 207 (1998).
17. I.S. Gradshteyn and I.M. Ryzhik. Table of integral, series, and products. Academic Press Inc., Orlando, Fla. 1980.
18. V. Bagini, R. Borghi, F. Gori, A.M. Pacileo, and M. Santarsiero. J. Opt. Soc. Am. A, **13**, 1385 (1996).
19. S.A. Amarande. Proc. SPIE, **3092**, 345 (1997).
20. M. Sasnett and K. Witting. Proc. SPIE, **2375**, 214 (1995).
21. T.F. Johnston, Jr. Laser Focus World, **173**, (1990).
22. S. Saghafi, M.J. Withford, and J.A. Piper. J. Opt. Soc. Am. A: Special edition on free and guided beams, **18**(7), 1634 (2001).